

# Charge and canted spin order in $\text{La}_{2-x}\text{Sr}_x\text{NiO}_4$ ( $x=0.275$ and $\frac{1}{3}$ )

S.-H. Lee,<sup>1,2</sup> S.-W. Cheong,<sup>3</sup> K. Yamada,<sup>4</sup> and C. F. Majkrzak<sup>1</sup>

<sup>1</sup>NIST Center for Neutron Research, National Institute of Standards and Technology, Gaithersburg, Maryland 20899

<sup>2</sup>University of Maryland, College Park, Maryland 20742

<sup>3</sup>Department of Physics and Astronomy, Rutgers University and Bell Laboratories, Lucent Technologies, Murray Hill, New Jersey 07974

<sup>4</sup>Kyoto University, Institute of Chemical Research, Uji 611-0011, Kyoto, Japan

(Received 30 October 2000; published 18 January 2001)

Polarized neutron diffraction on  $\text{La}_{2-x}\text{Sr}_x\text{NiO}_4$  ( $x=0.275$  and  $1/3$ ) reveals that the spins in the ordered phases are canted in the  $\text{NiO}_2$  plane away from the charge and spin stripe direction. The deviation angle is larger for  $x=1/3$  than for  $x=0.275$ . Furthermore, for the optimal  $x=1/3$  stoichiometry, an enhancement of the charge contribution and a larger canting of the spins occur below 50 K, which indicates a further lock in of the doped holes.

DOI: 10.1103/PhysRevB.63.060405

PACS number(s): 75.30.Fv, 71.45.Lr, 75.25.+z

The interplay between charge and spin degrees of freedom has been a central issue in doped antiferromagnets in connection with high temperature superconductivity.<sup>1-4</sup> When holes are doped into layered antiferromagnetic (AFM) insulators, the holes segregate into stripes which form antiphase domain walls between the intervening AFM regions. One dimensionality of the charge and spin modulations in superconducting cuprates has been evidenced in recent transport<sup>5</sup> and neutron scattering<sup>6,7</sup> measurements. A recent study on  $\text{La}_{1.6-x}\text{Nd}_{0.4}\text{Sr}_x\text{CuO}_4$  suggests that charge stripe correlations are prerequisite for superconductivity.<sup>8</sup>

The stripe phase was originally proposed to account for magnetic and nuclear superlattice peaks found in insulating  $\text{La}_{2-x}\text{Sr}_x\text{NiO}_{4+\delta}$  [LSNO].<sup>9,10</sup> Because of its strong electron-phonon interactions, the nickelate is a prototypical system for the understanding of charge and spin ordering. For hole concentrations  $n_h = x + 2\delta > 0.1$ , incommensurate (IC) reflections due to charge and spin ordering appear with the characteristic wave vectors  $Q_{\text{spin}} = (1 \pm \epsilon, 0, 0)$  and  $Q_{\text{charge}} = (2\epsilon, 0, 1)$  where  $\epsilon \approx n_h$ .<sup>9-12</sup> Commensurability effects have been reported for  $n_h \approx 1/3$  in various measurements indicating strong binding of charges to the lattice.<sup>12-14</sup> Recent resistivity measurements for the optimal  $n_h \approx 1/3$  showed that the charge stripes can be delocalized by an electric field.<sup>15</sup> For moderate electric fields, however, resistivity shows a sudden increase at low temperatures.

The main difficulty of studying the commensurability effect using neutron scattering techniques is that for  $\epsilon=1/3$  the charge and spin peaks coincide at the same wave vectors in  $Q$ -space. In this paper we report the first polarized neutron diffraction on LSNO ( $x=0.275$  and  $x=1/3$ ) which is a well-established technique to distinguish charge and spin contributions. Our results show that spins in the stripe phases are canted by an angle  $\theta$  from the stripe direction. The canted spin structure as the magnetic ground state for the nickelates represents a challenge for all theories of the stripe phase. The deviation angle  $\theta$  is larger for the higher hole concentration  $x$ :  $\theta(x=0.275)=27(7)^\circ$  below  $T_N=155(5)$  K and  $\theta(x=1/3)=40(3)^\circ$  for  $50 \text{ K} < T < T_N=200(10)$  K. Furthermore, for  $x=1/3$  another phase transition occurs at 50 K involving a further localization of charge and a larger canting of spins to

$\theta=53(3)^\circ$ . This indicates that the lower  $T$  charge stripe phase with large pinning potential is responsible for the anomalous robustness of the charge stripes found in the resistivity measurements.

A 10 g LSNO ( $x=0.275$ ) and two LSNO ( $x=1/3$ ) crystals with weight of 3.5 g and 15 g were grown for this work by the floating-zone method at Kyoto University and at Bell Laboratories, respectively. The crystal structure of both materials remains tetragonal with the  $I4/mmm$  symmetry over the range of temperature,  $10 \text{ K} < T < 320 \text{ K}$ , with  $a_t = 3.82(1) \text{ \AA}$  and  $c = 12.64(5) \text{ \AA}$  at 11 K for  $x=0.275$  and with  $a_t = 3.83(1) \text{ \AA}$  and  $c = 12.69(5) \text{ \AA}$  at 11 K for  $x=1/3$ . For convenience, however, we use orthorhombic lattice units with  $a_o = \sqrt{2}a_t$  which is rotated by  $45^\circ$  with respect to the Ni-O bonds in the  $\text{NiO}_2$  planes.

Neutron-scattering measurements were performed on the cold neutron triple axis spectrometer SPINS at NIST. The incident neutron energy was  $E_i = 5 \text{ meV}$  and higher-order contamination was eliminated by a cryostat-cooled Be filter before the sample. The incident neutrons were polarized in one spin state by a forward transmission polarizer. The spin state of the scattered neutrons from the sample was then analyzed with a rear flipper and polarizer combination. A collimator was placed right after each polarizer to eliminate the other spin state. The samples were mounted in such a way that the  $(h0l)$  reciprocal plane becomes the scattering plane. A guide field was applied vertically along the  $(010)$  axis. Collimations were guide-40-40-open for the LSNO( $x=0.275$ ) measurements and guide-40-20-open for the LSNO( $x=1/3$ ) measurements. The polarizing efficiency was 0.89(1) for the former and 0.90(1) for the latter. In this geometry, the spin component parallel with the guide field and the nuclear structural component contribute to non-spin-flip (NSF) channel whereas the spin component normal to  $\vec{Q}$  in the scattering plane contributes to the spin-flip (SF) channel. Since spins in the nickelates are coplanar in  $ab$  plane,<sup>16,17</sup> the NSF and SF neutron-scattering cross sections for  $Q=(h0l)$ ,  $\sigma_{\text{NSF}}(Q)$  and  $\sigma_{\text{SF}}(Q)$  respectively, can be written as<sup>18</sup>

$$\sigma_{\text{NSF}}(Q) = \sigma_N(Q) + \sigma_M^b(Q)$$

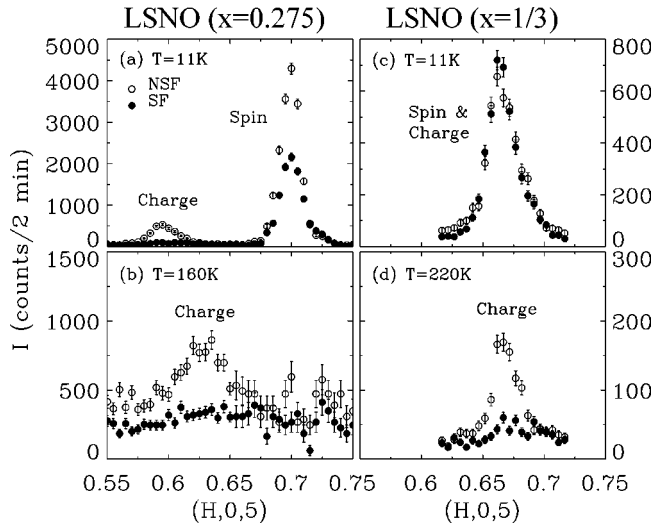


FIG. 1. Polarized elastic neutron scattering data along ( $h05$ ) from LSNO( $x=0.275$ ) [(a) and (b)], and from LSNO( $x=1/3$ ) [(c) and (d)].

$$\sigma_{SF}(Q) = \sigma_M^a(Q) \left[ 1 - \frac{(ha^*)^2}{(ha^*)^2 + (lc^*)^2} \right], \quad (1)$$

where  $\sigma_N$  is the structural scattering cross section, and  $\sigma_M^a$  and  $\sigma_M^b$  are the  $a$  and  $b$  components of the magnetic scattering cross section, respectively. Here, in  $\sigma_{NSF}$ , the interference term between the structural and the magnetic scattering was neglected because for the  $x=1/3$  sample the two NSF scattering intensities,  $\sigma(- -)$  and  $\sigma(+ +)$ , were the same within the experimental accuracy for all the superlattice reflections considered in the paper.

Figure 1 shows the results of polarized neutron diffraction on LSNO( $x=0.275$  and  $1/3$ ). For  $x=0.275$ , at 11 K the data exhibit two types of superlattice peaks: the first harmonic at  $(0.7,0,5)$  separated by  $(\epsilon,0,0)$  from the  $(105)$  AFM Bragg reflection in pure  $\text{La}_2\text{NiO}_4$  and the second harmonic at  $(0.6,0,5)$  separated by  $(2\epsilon,0,1)$  from the  $(004)$  nuclear Bragg reflection with  $\epsilon=0.3 \approx x$ .<sup>12</sup> The first harmonic has both NSF and SF components whereas the second harmonic has a NSF component only. This directly confirms that the first harmonic is magnetic (spin peak) whereas the second harmonic is nonmagnetic (charge peak) in origin. We can estimate the degree of local lattice distortion due to charge ordering in LSNO ( $x=0.275$ ) by comparing the intensities at  $(0.6,0,5)$  and at  $(0.7,0,5)$ :  $\sigma_{NSF}(0.6,0,5)/\sigma_{NSF}(0.7,0,5) = 0.12(1)$ . As shown in Fig. 3(a), the charge peak gradually increases below  $T_c$  and then get enhanced in a weakly first order at  $T_s$  when spins order. Inplane charge correlation length,  $\xi_c$ , also increases at  $T_s$ . In the charge and spin ordered phase the charge peak is broader than the spin peak, indicating that  $\xi_c$  is shorter than inplane spin correlation length,  $\xi_s$ :  $\xi_c/\xi_s \approx 100 \text{ \AA}/300 \text{ \AA} = 1/3$  [see the inset of Fig. 3(a)]. It has been argued<sup>19</sup> that disorders in the stripes are mostly due to non-topological elastic deformations along the stripes and the decrease of the correlation lengths is inversely proportional to a power of the periodicity, which can explain why  $\xi_c$  is smaller than  $\xi_s$  even though the charge and spin correlations

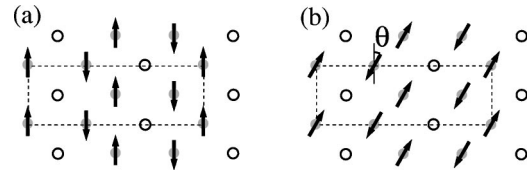


FIG. 2. Possible spin structures in a  $\text{NiO}_2$  plane for LSNO( $x=1/3$ ). Open and filled circles represent nickel ions with and without holes, respectively. (a) Spins are perpendicular to the propagation vector along the  $(100)$  axis. (b) Spins are uniformly canted by an angle  $\theta$  from the  $(010)$  axis. Dashed lines indicate the magnetic unit cell.

are inexorably connected. For comparison,  $\xi_c/\xi_s = 1/4$  for  $\text{La}_{1.6-x}\text{Nd}_{0.4}\text{Sr}_x\text{CuO}_4$ .<sup>20</sup> As shown in Figs. 1(a) and 1(b), upon heating the  $(0.7,0,5)$  and  $(0.6,0,5)$  superlattice peaks shift toward  $(\frac{2}{3},0,5)$  until the  $(0.7,0,5)$  peak vanishes at 155(5) K and the  $(0.6,0,5)$  peak at 200(10) K [see Fig. 3(a)]. In the intermediate temperature range ( $155 \text{ K} < T < 200 \text{ K}$ ), as shown in Fig. 1(b), the charge order exists without the spin order. For  $x=1/3$ , at 11 K the first and second harmonics with  $\epsilon=x$  come together at the same wavevector as shown in Fig. 1(c). Unlike the case for  $x=0.275$ , the position of the superlattice peak for  $x=1/3$  is independent of  $T$ , implying the stability of commensurability.<sup>21</sup> At 220 K, the  $(2/3,0,5)$  peak has a NSF component only, indicating that the  $x=1/3$  system also has an intermediate  $T$  phase with charge order only.

Besides identifying the origins of the scattering, polarized neutron diffraction data can also determine the spin structure. Due to crystal twinning, the stripe order produces a four-fold pattern along  $(100)$  (twin No. 1 with  $a^*/(100)$ ) and  $(010)$  (twin No. 2 with  $a^*/(010)$ ) directions around the magnetic reciprocal lattice position. Since the stripe propagates along  $a^*$ , the  $(h01)$  superlattice reflections originate from twin No. 1 only.<sup>7</sup> Since the spin peaks having SF as well as NSF scattering indicates both  $\sigma_M^a=0$  and  $\sigma_M^b$  are non-zero, the moments are canted in the  $ab$  plane away from the  $(100)$  stripe direction. The spin structure shown in Fig. 2(a) can therefore be ruled out as magnetic ground state for the nickelates. For quantitative studies, the NSF and SF scattering have been measured at various superlattice reflections and at different temperatures. Fig. 3(b) shows some of the results for  $x=1/3$ . Upon cooling, NSF scattering at the  $(2/3,0,5)$  reflection develops at 240 K without SF scattering, indicating charge ordering. Below around 200 K, SF as well as NSF scattering increases due to spin ordering in the usual second-order fashion. At 50 K, however, the trend changes: the NSF scattering decreases whereas the SF increases. This behavior can be more clearly seen in the ratio of SF to NSF scattering shown in Fig. 3(c). The sharp increase in the ratios below 50 K indicates that the phase transition at 50 K involves reorientation of spins. For  $x=0.275$ , the SF to NSF ratios of the spin peak in the spin-ordered phase were smaller than those for the corresponding reflections in the  $x=1/3$  system and no spin reorientation transition was observed down to 10 K.

The symbols in Fig. 4 summarize the measured  $\sigma_{SF}/\sigma_{NSF}$  for LSNO( $x=0.275$ ) and for the two spin-ordered phases in LSNO( $x=1/3$ ). The data show a general trend: for a given

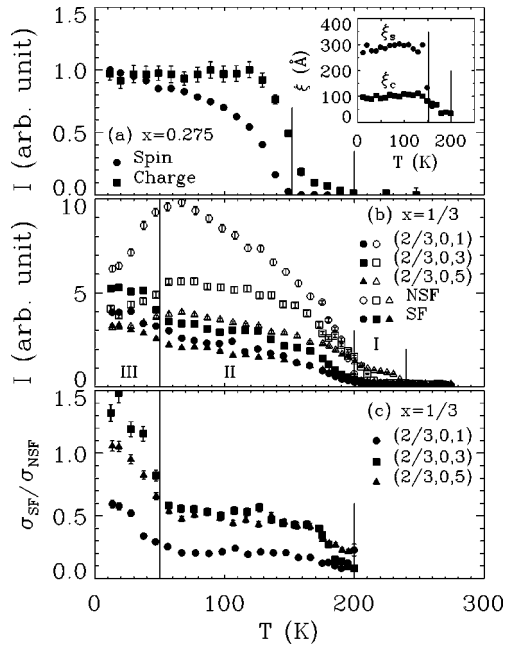


FIG. 3. (a)  $T$  dependence of unpolarized elastic neutron scattering intensities of the charge peak and the spin peak. (b) NSF (open symbols) and SF (filled symbols) scattering intensities at various superlattice reflections from LSNO( $x=1/3$ ) as a function of  $T$ . (c)  $T$  dependence of the ratio of SF to NSF scattering intensities after backgrounds were determined above the transition temperature and subtracted.

value of  $h$  in each phase,  $\sigma_{SF}/\sigma_{NSF}$  increases as  $l$  increases with an exception at the  $(2/3, 0, 5)$  reflection for  $x=1/3$ . The deviation of the  $(2/3, 0, 5)$  reflection is due to the fact that the  $(2/3, 0, 5)$  peak has a charge component as well as spin component. Our unpolarized neutron-scattering data along  $(0.6, 0, 0 \leq l \leq 5)$  on the  $x=0.275$  sample have the strongest intensity at  $l=5$  but negligible at other  $l$ , indicating the structure factor due to charge ordering is strong at  $(0.6, 0, 5)$  but not at other  $l$ . We expect the same holds for  $x=1/3$ .

Now consider the canted spin structure shown in Fig. 2(b). Since the spins have a  $b$  component, SF scattering

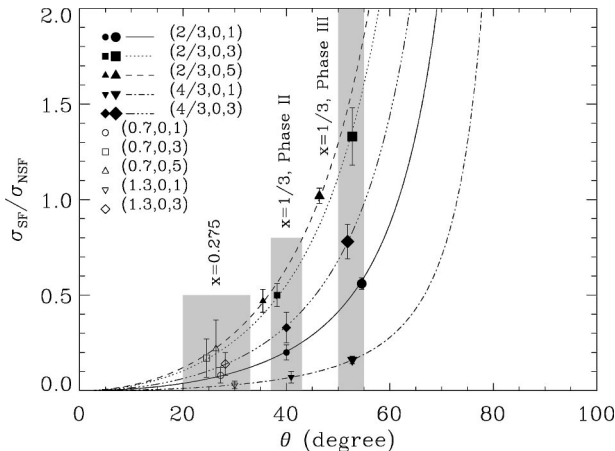


FIG. 4. Experimental (symbols) and the model calculated (lines) ratios of SF to NSF scattering cross sections as a function of the rotation angle  $\theta$ .

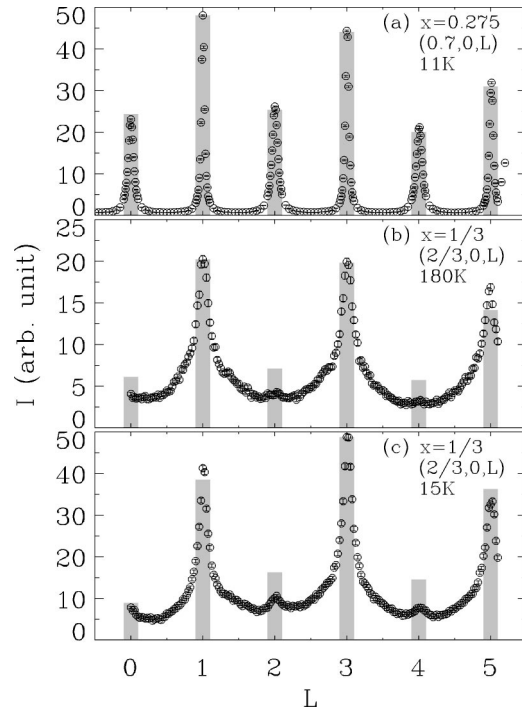


FIG. 5.  $l$  dependence of (a)  $(0.7, 0, l)$  scan from LSNO ( $x=0.275$ ) at 11 K, and  $(2/3, 0, l)$  scan from LSNO( $x=1/3$ ) (b) at 180 K and (c) 15 K. The shaded bars are obtained by the model which is described in the text.

would be nonzero and the ratio of SF to NSF scattering would be determined by the angle  $\theta$ . The lines in Fig. 4 are the calculated  $\sigma_{SF}/\sigma_{NSF}$  for the canted spin structure assuming  $\sigma_N=0$ :

$$\frac{\sigma_{SF}}{\sigma_{NSF}} = \tan^2 \theta \cdot \left( 1 - \frac{(ha^*)^2}{(ha^*)^2 + (lc^*)^2} \right). \quad (2)$$

From the comparison to the data, we conclude that  $\theta=27^\circ \pm 7^\circ$  for  $x=0.275$ ,  $40^\circ \pm 3^\circ$  for phase II and  $52.5^\circ \pm 2.5^\circ$  for phase III in the  $x=1/3$  sample. The  $(2/3, 0, 5)$  reflection deviates from the model due to large charge contribution. It is to be emphasized that the deviation is more pronounced in phase III than in phase II. Using Eq. (1) and (2), we can estimate the charge contribution in the  $(2/3, 0, 5)$  reflection to be  $\sigma_N/\sigma_M^b = 0.36(6)$  (phase II) and  $0.52(4)$  (phase III). This indicates a further localization of the doped holes in phase III than in phase II. In recent resistivity measurements on LSNO ( $n_h \approx 1/3$ ),<sup>15</sup> at intermediate temperatures a moderate inplane electric field ( $V_{cir} \geq 100$  V) delocalizes the charge stripes. At low temperatures, however, the charge stripes survive until  $V_{cir} \geq 900$  V. The robustness of charge stripes at low  $T$  is due to the large pinning potential of charge stripes in phase III.

Unpolarized neutron-diffraction data along the  $l$  direction also contain information on spin structure. As shown in Fig. 5, the peaks are much sharper in  $l$  for  $x=0.275$  than for  $x=1/3$ , which indicates that the correlations in  $x=0.275$  are nearly three-dimensional whereas those in  $x=1/3$  are quasi-two-dimensional. Another obvious difference between them is that the even  $l$  to odd  $l$  peak intensity ratio,

$I(\text{even } l)/I(\text{odd } l)$ , is much larger for  $x=0.275$  than for  $x=1/3$ . There are other subtle features to be noted. For  $x=0.275$ , the odd  $l$  peak weakens as  $l$  increases whereas the even  $l$  peak is strongest at  $l=2$ . For  $x=1/3$ , at 180 K (phase II) the odd  $l$  peak also weakens as  $l$  increases. However at 15 K (phase III) the  $l=3$  peak becomes strongest. If the uncanted spin structure of Fig. 2(a) is displaced by  $(a/2n, 1/2, 1/2)$  with integer  $n$  in neighboring  $\text{NiO}_2$  planes, the magnetic neutron-scattering cross section would become  $\sigma(Q) \propto |F(Q)|^2 [1 + (-)^l \cos n\pi h]$  (Ref. 22) where  $F$  is the magnetic form factor of the  $\text{Ni}^{2+}$ . Therefore, for a given  $h$ , the  $l$  dependence of odd or even  $l$  peaks would just follow  $|F(Q)|^2$ . This  $\sigma(Q)$  cannot explain those subtle features. On the other hand, the canted spin structure of Fig. 2(b) would give

$$\sigma(Q) \propto |F(Q)|^2 [1 + (-)^l \cos n\pi h] \times \left[ 1 - \sin^2 \theta \frac{(ha^*)^2}{(ha^*)^2 + (lc^*)^2} \right]. \quad (3)$$

With the  $\theta$ 's which are obtained from the polarization analysis, Eq. (3) reproduces the  $l$  dependence remarkably well for the case of  $x=0.275$  with three-dimensional magnetic correlations, as shown as shaded bars in Fig. 5. In the case of  $x=1/3$  where the magnetic order is quasi-two-dimensional, the long tails of the peaks make it difficult to extract the integrated intensities to compare with the model. Neverthe-

less, the model explains the subtle features such as the  $(2/3, 0, 3)$  peak being considerably stronger than the other reflections in phase III.

In summary, charge ordering plays the dominant role for the electronic and magnetic properties in the nickelates. Our polarization analysis on LSNO ( $x=0.275$  and  $1/3$ ) has shown that is not only charge order prerequisite for magnetic order, but also it determines local magnetic order. The ground state of the local magnetic order in these materials turns out to be the canted spin structure in the  $\text{NiO}_2$  plane rather than the uncanted spin structure that has been assumed for the nickelates.<sup>9</sup> Both local lattice distortion due to charge ordering and the canting angle of spins are larger for  $x=1/3$ , indicating stability of the commensurate charge stripe order. For  $x=1/3$ , below 50 K occur an increased pinning of the charge stripes to the lattice and a larger canting of the spins. Understanding whether or not the canted spin order is the ground state in general for doped nickelates and cuprates would require more studies and provide important information on the interconnection between charge, lattice and spin correlations in the doped antiferromagnets.

The authors thank G. Aeppli, J.M. Tranquada, G. Shirane, C. Brown, Y.S. Lee, and S. Wakimoto for helpful discussions. Work at SPINS is based upon activities supported by the National Science Foundation under Agreement No. DMR-9423101.

<sup>1</sup>V. J. Emery, S. A. Kivelson, and J. M. Tranquada, Proc. Natl. Acad. Sci. **96**, 8814 (1999), and references therein.

<sup>2</sup>S.-W. Cheong *et al.*, Phys. Rev. Lett. **67**, 1791 (1991).

<sup>3</sup>J. M. Tranquada *et al.*, Nature **375**, 561 (1995); Phys. Rev. Lett. **78**, 338 (1997).

<sup>4</sup>K. Yamada *et al.*, Phys. Rev. B **57**, 6165 (1998).

<sup>5</sup>T. Noda *et al.*, Science **286**, 265 (1999).

<sup>6</sup>S. Wakimoto *et al.*, Phys. Rev. B **61**, 3699 (2000).

<sup>7</sup>H. A. Mook *et al.*, Nature **404**, 729 (2000).

<sup>8</sup>N. Ichikawa *et al.*, Phys. Rev. Lett., in press (2000).

<sup>9</sup>J. M. Tranquada *et al.*, Phys. Rev. Lett. **73**, 1003 (1994); Phys. Rev. B **52**, 3581 (1995); **54**, 12 318 (1996).

<sup>10</sup>C. H. Chen *et al.*, Phys. Rev. Lett. **71**, 2461 (1993).

<sup>11</sup>S. M. Hayden *et al.*, Phys. Rev. Lett. **68**, 1061 (1992).

<sup>12</sup>H. Yoshizawa *et al.*, Phys. Rev. B **61**, R854 (2000).

<sup>13</sup>T. Katsufuji *et al.*, Phys. Rev. B **54**, R14230 (1996).

<sup>14</sup>K. Yamamoto *et al.*, Phys. Rev. Lett. **80**, 1493 (1998); T. Katsufuji *et al.*, Phys. Rev. B **60**, R5097 (1999).

<sup>15</sup>S. Yamanouchi *et al.*, Phys. Rev. Lett. **83**, 5555 (1999).

<sup>16</sup>G. Aeppli *et al.*, Phys. Rev. Lett. **61**, 203 (1988).

<sup>17</sup>Our polarized neutron-diffraction measurements on the LSNO( $x=1/3$ ) sample in the  $(hk0)$  scattering plane confirmed that the spins lie in the  $ab$ -plane.

<sup>18</sup>R. M. Moon *et al.*, Phys. Rev. **181**, 920 (1969).

<sup>19</sup>O. Zachar, cond-mat/9911171, Phys. Rev. B (to be published).

<sup>20</sup>J. M. Tranquada *et al.*, Phys. Rev. B **59**, 14 712 (1999).

<sup>21</sup>S.-H. Lee and S.-W. Cheong, Phys. Rev. Lett. **79**, 2514 (1997).

<sup>22</sup>P. Wochner *et al.*, Phys. Rev. B **57**, 1066 (1998).